

# Impedance spectroscopy and nanoindentation of conducting poly(3,4-ethylenedioxythiophene) coatings on microfabricated neural prosthetic devices

Junyan Yang<sup>a)</sup>

*Department of Materials Science and Engineering, University of Michigan, Ann Arbor, Michigan 48109-2136*

David C. Martin<sup>b)</sup>

*Departments of Materials Science and Engineering, and Biomedical Engineering, and Macromolecular Science and Engineering Center, University of Michigan, Ann Arbor, Michigan 48109-2136*

(Received 21 September 2005; accepted 16 December 2005)

The electrical and mechanical properties of conducting polymer poly(3,4-ethylenedioxythiophene) coatings on microfabricated neural probes have been evaluated by electrochemical impedance spectroscopy and nanoindentation techniques. Our results reveal that for poly(3,4-ethylenedioxythiophene) coatings, the minimum impedance correlates well with the mechanical properties. The lowest impedance films are also those that are the softest. This is consistent with microstructural observations by atomic force microscopy and scanning electron microscopy showing an increase in the effective surface area (“fuzziness”) of the coatings. The presence of these conducting polymer coatings provides an intermediate step along the interface between the devices and brain tissue. This information provides clues for the design of strategies for improving the long-term performance of these electrodes in vivo.

## I. INTRODUCTION

Microfabricated silicon-based neural prosthetic devices facilitate the functional stimulation of and recording from neurons of the central nervous system. The bulk modulus of silicon is  $\sim 170$  GPa, whereas a value of  $\sim 0.1$  MPa for the modulus of human brain was obtained.<sup>1</sup> This corresponds to a 7-order of magnitude difference between the modulus of devices and brain tissue. This may lead to local strains at the sample surface during chronic implantations in living tissue that could enhance glial cell inflammation and thus reduce the biocompatibility of the device. The conducting polymer poly(3,4-ethylenedioxythiophene) (PEDOT) has been used for biomedical applications because of its excellent long-term stability and relatively high transparency.<sup>2,3</sup> This material exhibits significantly better electrical conductivity and chemical stability than polypyrrole (PPy).<sup>4</sup> In our laboratory, we have been investigating the use of conducting PEDOT coatings for improving the long-term performance of microfabricated neural prosthetic devices that are directly implanted into the central nervous

system. We have found that soft, low impedance, and biologically active conducting PEDOT coatings can be prepared by electrochemical deposition on the electrode sites.<sup>5</sup> More recently, we also have explored a number of methods to create features of well-defined size and high surface area in nanostructured conducting PEDOT thin films using templating and surfactant-mediated techniques.<sup>6–8</sup> By correlating measurements of probe electrical properties with their surface morphologies, we have found that maximizing the effective surface area of the electrode coating makes it possible to minimize the electrical impedance. This is consistent with the interpretation that the high surface area of the films promotes the most facile charge transport.

The presence of conducting polymer thin films on neural probes can provide an intermediate step along the interface between the devices and brain tissues. However, the conducting polymer thin films may have different mechanical properties from the bulk. To monitor the coating property changes with polymerization condition, methods of mechanical testing with the ability to characterize surface properties on a micron to nanometer scale spatial resolution are required. There are a number of methods for measuring the mechanical properties (hardness, stiffness, and modulus) of polymer thin films or coatings on substrates, such as peeling, scratching,

<sup>a)</sup>Present address: Dow Chemical Company, Freeport, TX 77541

<sup>b)</sup>Address all correspondence to this author.

e-mail: milty@umich.edu  
DOI: 10.1557/JMR.2006.0145

stretching, and microhardness. For example, the mechanical properties of  $\sim 100\text{-}\mu\text{m}$ -thick polythiophene,<sup>9</sup> PPy,<sup>10</sup> and PEDOT composites<sup>11</sup> have been investigated by means of stress-strain tests. Significant evidence for the effects of film thickness and the electrochemical polymerization conditions on mechanical properties were found. Our conducting PEDOT coatings are directly deposited on neural probes and are typically less than  $10\ \mu\text{m}$  thick; in many cases, they are less than  $1\ \mu\text{m}$ . In addition, these coatings are deposited on the electrode sites that are only  $\sim 40\ \mu\text{m}$  in diameter, so it is considerably more difficult to obtain mechanical profiles of these small amounts of conducting polymer using traditional testing techniques. Nanoindentation is a relatively new technique that relies on the local deformation of a materials surface using an indenter with a known geometry under the application of a given load. This method is particularly suited for thin films. It has been used to generate information about the deformation behavior of a number of polymer thin films, coatings, blends, and composites.<sup>12–15</sup> However, few studies of conducting polymer thin films have yet been presented.

This article evaluates the mechanical properties of conducting polymer PEDOT coatings by using nanoindentation and compares them with their electrical properties. The morphological structures in the film were examined with scanning electron microscopy (SEM) and atomic force microscopy (AFM).

## II. EXPERIMENTAL

3,4-ethylenedioxythiophene (EDOT,  $>97\%$ ) monomer was obtained from Bayer AG (Elkhart, IN). Lithium perchlorate ( $\text{LiClO}_4$ ) was purchased from Aldrich (Milwaukee, WI) and was used without any previous purification. Microfabricated neural probes with gold-coated eight sites along the shank ( $1256\ \mu\text{m}^2$  in area per site) were provided by the University of Michigan Center for Neural Communication Technology.

The PEDOT/ $\text{LiClO}_4$ -conducting polymer coating was electrochemically polymerized directly on the electrode sites under galvanostatic conditions at room temperature using a current density of  $0.5\ \text{mA}/\text{cm}^2$  in an aqueous solution of  $0.01\ \text{M}$  EDOT and  $0.01\ \text{M}$   $\text{LiClO}_4$ . The electrical supply was an Autolab potentiostat/galvanostat PGStat12 (EcoChimie, Utrecht, The Netherlands). The electrochemical polymerization was performed in a conventional three-electrode cell. A platinum foil was used as the counter electrode, a saturated calomel electrode was used as the reference electrode, and the probe sites were used as the working electrode. The amount of polymer coated on the electrode site (film thickness) was controlled by the total charge passed during polymerization. After the electrochemical deposition was completed, the electrode probes were washed with deionized water to remove any residual monomer or counterions.

An electrochemical impedance system (AutoLab potentiostat/galvanostat; EcoChimie) was used to obtain electrochemical impedance spectra (EIS) of PEDOT-coated electrodes. A solution of  $0.1\ \text{M}$  phosphate-buffered solution (pH 7) was used as the electrolyte in the cell. The impedance spectra were recorded at 15 discrete frequencies over a frequency range from  $1\ \text{Hz}$  to  $100\ \text{kHz}$ . The charge capacity of PEDOT-coated electrodes was measured by means of cyclic voltammetry (CV). CV was performed with the same instrument as EIS by sweeping between  $-0.9$  to  $+0.5\ \text{V}$  versus saturated calomel electrode, with a scan rate of  $100\ \text{mV}/\text{s}$ . Five eight-site gold-coated probes were tested under the same conditions. Each time, we measured the impedance and CV at least four times. The impedance at  $1\ \text{kHz}$  was examined in detail because this frequency corresponds to the characteristic temporal width of a typical neural signal.

A Nano II (Nano Instruments, Oak Ridge, TN) was used to perform the nanoindentation tests. A pyramidal-shaped (Berkovitch) diamond tip ( $65.3^\circ$  angle) was progressively pressed onto the same surface by a  $\mu\text{N}$ -scale force (maximum force of  $900\ \text{mN}$ ). A series of five indentations (indentation spacing:  $5\ \mu\text{m}$ ) were performed for each site, and the results were averaged to generate a mean load-displacement curve. A quartz standard sample was used to calibrate the instrument and calculate the tip area function.

Optical microscopy was conducted with a Optiphot POL (Nikon, Melville, NY), having the capability for reflected and transmitted light observations. Images were acquired with a Spot RT digital camera running on a computer workstation (Dell, Round Rock, TX). SEM micrographs were taken by using a XL30 (Philips, Eindhoven, The Netherlands) with a typical voltage of  $5\ \text{kV}$ . AFM images of PEDOT coatings on the electrode sites were obtained with a Nanoscope III with a multimode head (Digital Instruments, Santa Barbara, CA). Surface scans from the AFM were analyzed using NanoScope III software (version 5.12r3; Digital Instruments). Characteristic analyses of the sample surface profiles were obtained.

## III. RESULTS AND DISCUSSION

### A. PEDOT-coated electrode probes

Optical micrographs such as those shown in Fig. 1 confirmed that conducting polymer PEDOT coatings doped with  $\text{LiClO}_4$  could be electrochemically deposited on the sites of neural probe under galvanostatic conditions. The PEDOT/ $\text{LiClO}_4$  was formed directly over the conducting site ( $40\ \mu\text{m}$  in diameter) and was dark blue/black in color. Figure 2 shows SEM micrographs of the top view of PEDOT/ $\text{LiClO}_4$  films electrochemically deposited on the electrode sites as a function of deposition charge under galvanostatic conditions. In this case, the

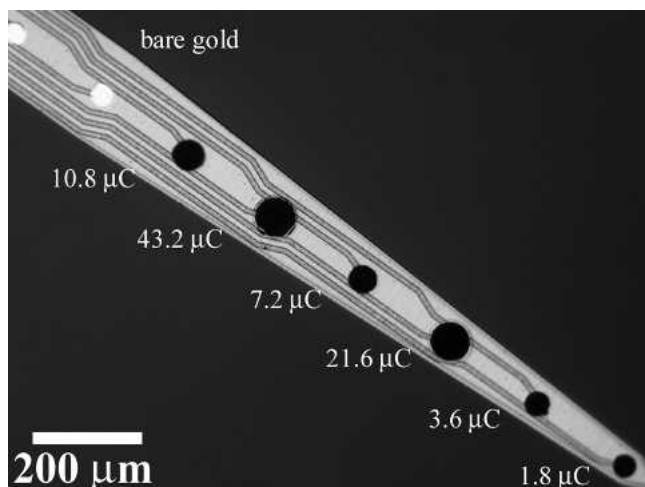


FIG. 1. Optical micrograph of conducting PEDOT/LiClO<sub>4</sub>-coated eight-site neural probe (inset numbers show deposition charge). The concentration of EDOT and LiClO<sub>4</sub> was 0.01 M, and the growth current density is 0.5 mA/cm<sup>2</sup>.

current density during the polymerization was controlled at 0.5 mA/cm<sup>2</sup>. As can be seen from Fig. 2, the PEDOT coatings grew in thickness as the deposition charge increased, and further spread out of the sites at higher deposition charge. The thickness of the coatings could be roughly estimated from the side view of optical micrographs using National Institutes of Health image software and could then be measured accurately from side view SEM images using Photoshop software (Adobe Systems, Mountain View, CA). It can be seen from Fig. 3 that the thickness of PEDOT coatings increased systematically with the deposition charge. With EDOT and LiClO<sub>4</sub> concentrations of 0.01 M, and a current density of 0.5 mA/cm<sup>2</sup> for electrochemical polymerization, a 4- $\mu\text{m}$  thickness coating was deposited on a 1256- $\mu\text{m}^2$  site with a deposition charge of approximately 11  $\mu\text{C}$  (or a deposition time of 30 min). Therefore, we can easily control the amount of PEDOT coatings on the electrodes by the deposition charge.

To characterize the surface topography as the film grows, AFM was performed on a PEDOT/LiClO<sub>4</sub>-coated eight-site electrode probe as a function of the total deposition charge. Figure 4 shows AFM images of PEDOT/LiClO<sub>4</sub>-coated sites with increasing deposition charge from Figs. 4(a) to 4(f). The surface appeared to be composed of round globular particles, and the average globule diameter increased with increasing of the coating thickness (Fig. 5). Figure 5 shows that for a film with a nominal thickness of 1.7  $\mu\text{m}$  (deposition charge of 1.8  $\mu\text{C}$ ), the surface contained small globules, and the average size of the globule was only 0.05  $\mu\text{m}$ . As the film grew thicker than 6  $\mu\text{m}$  (deposition charge of 22  $\mu\text{C}$ ), the size of the globules increased to 0.13  $\mu\text{m}$  [Fig. 5(e)]. The globule size increased to 0.2  $\mu\text{m}$  for a film thickness of 10  $\mu\text{m}$  (deposition charge of 43  $\mu\text{C}$ ).

## B. Electrical properties

The impedance and charge capacity of PEDOT-coated electrodes were measured by EIS and CV. Figure 6 shows the impedance spectra of a series of PEDOT-coated electrodes as a function of deposition charge in comparison with the uncoated gold electrode. The PEDOT-coated electrodes showed lower impedances over the whole frequency range of 1 Hz to 100 kHz than those of uncoated gold electrode. The impedance decreased with increasing frequency in low frequency range, reaching a minimum between 2 and 3 kHz, and then increased slightly at the higher frequency range. In addition, the impedance of the PEDOT-coated electrodes over the whole frequency range (1–100 kHz) decreased with increasing deposition charge. Furthermore, the amount of stored charge (charge capacity) of the PEDOT-coated electrodes increased approximately linearly with deposition charge (Fig. 7). Our previous results have shown that the higher effective surface area of PEDOT-coated electrodes is responsible for the decreased impedance and the improved charge capacity. Surfactant-templated-ordered PEDOT has a higher charge capacity than that of nodular PEDOT or nodular PPy at the same deposition charge because the charge capacity was affected by the surface morphology.<sup>8</sup>

## C. Nanoindentation measurement

The mechanical properties of conducting PEDOT-coated electrode were characterized using nanoindentation. In the nanoindentation measurement, a pyramidal-shaped (Berkovitch) diamond tip was progressively pressed onto the sample surface with a  $\mu\text{N}$ -scale force, which initiated the loading cycle. After reaching the maximum indentation depth, the tip was gradually removed from the sample, which initiated the unloading cycle, leaving behind an indentation on the sample surface. The indent depth and the stiffness of the measured material were recorded, and the mechanical properties such as hardness and modulus of the thin films were calculated. The apparent plastic hardness ( $H$ ) of the films was calculated by dividing the maximum applied load ( $P_{max}$ ) at a given displacement ( $h$ ) by the contact area ( $A$ ) of the resulting indent

$$H = P_{max}/A \quad ,$$

where the contact area is a function of displacement and is determined according to the following form

$$A(h) = 24.5 h^2 \quad .$$

A constant of 24.5 was used because it is assumed that a Berkovitch indenter has a perfect tip.<sup>16</sup> The effective elastic modulus (stiffness,  $S$ ) was also calculated from the unloading portion of the curves. Stiffness is defined as:

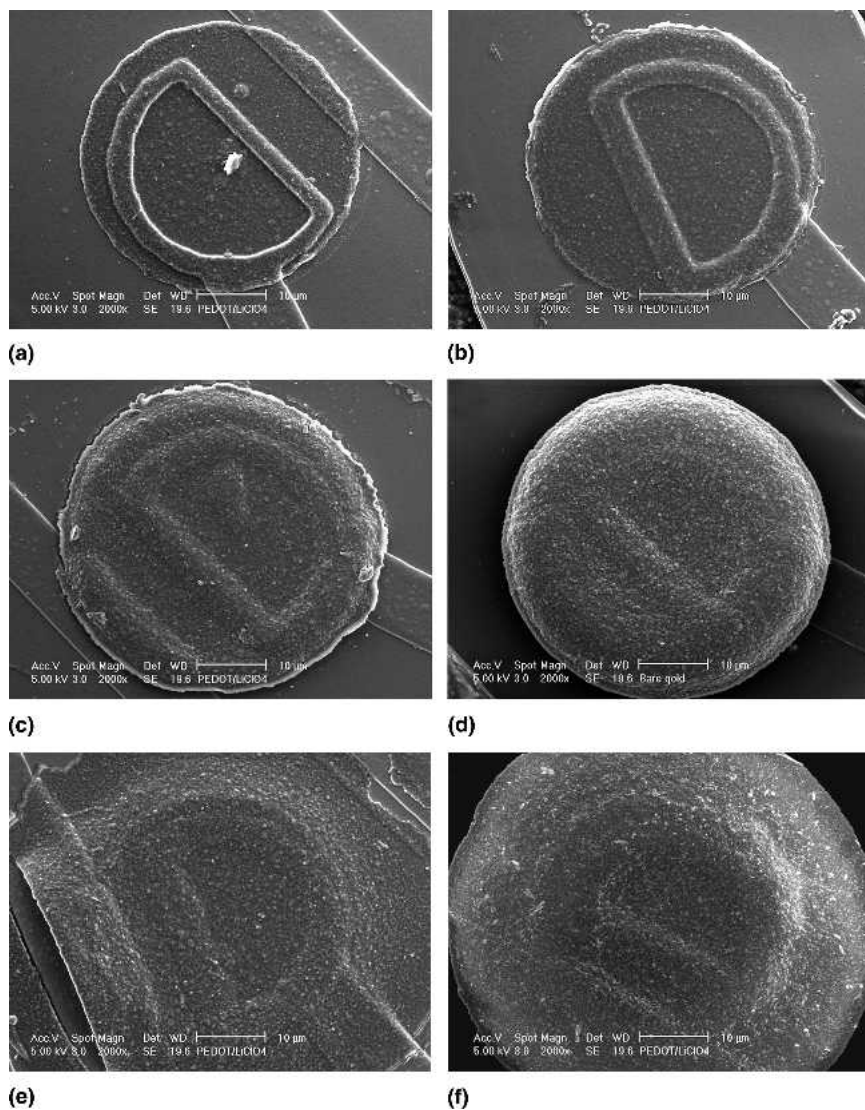


FIG. 2. SEM micrographs of PEDOT/LiClO<sub>4</sub> coatings deposited on gold-coated sites with deposition charge from (a) to (f) of 1.8 μC, 3.6 μC, 7.2 μC, 10.8 μC, 21.6 μC, and 43.2 μC. The concentration of EDOT and LiClO<sub>4</sub> was 0.01 M, and the growth current density was 0.5 mA/cm<sup>2</sup>.

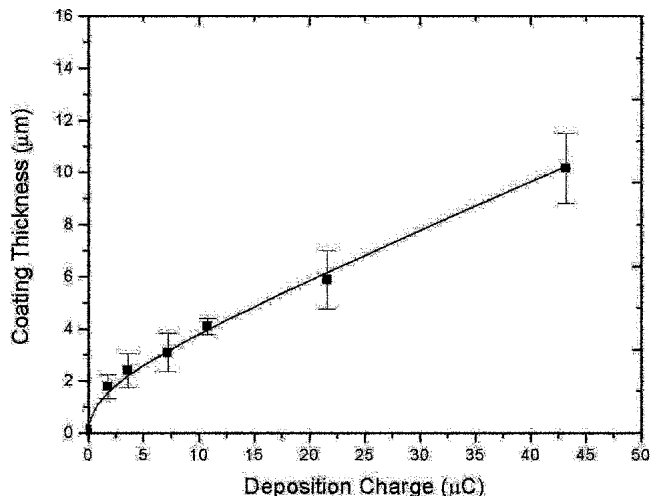


FIG. 3. The relationship between the PEDOT/LiClO<sub>4</sub> coating thickness and deposition charge.

$$S = dP/dA$$

Figure 8(a) shows typical load-displacement curves for a variety of PEDOT-coated electrodes under the same maximum load of 1 mN. The two main steps, loading cycle and unloading cycle, are noted in these figures. There are three important parameters in these figures: maximum load ( $P_{max}$ ), maximum displacement ( $h_{max}$ ), and plastic deformation ( $h_p$ , displacement from origin to the end point of unloading cycle). For example, for the PEDOT-coated electrode site obtained by passing through a deposition charge of 3.6 μC (or 10 min), the  $P_{max}$ ,  $h_{max}$ , and  $h_p$  are 0.92 mN, 548 nm, and 512 nm, respectively. The AFM image of this indent is shown in Fig. 8(b). The triangular shape left by the Berkovich indenter can be clearly seen. The section analysis under the image illustrates an indentation depth of 520 nm, which is consistent with the plastic deformation data ( $h_p$ )

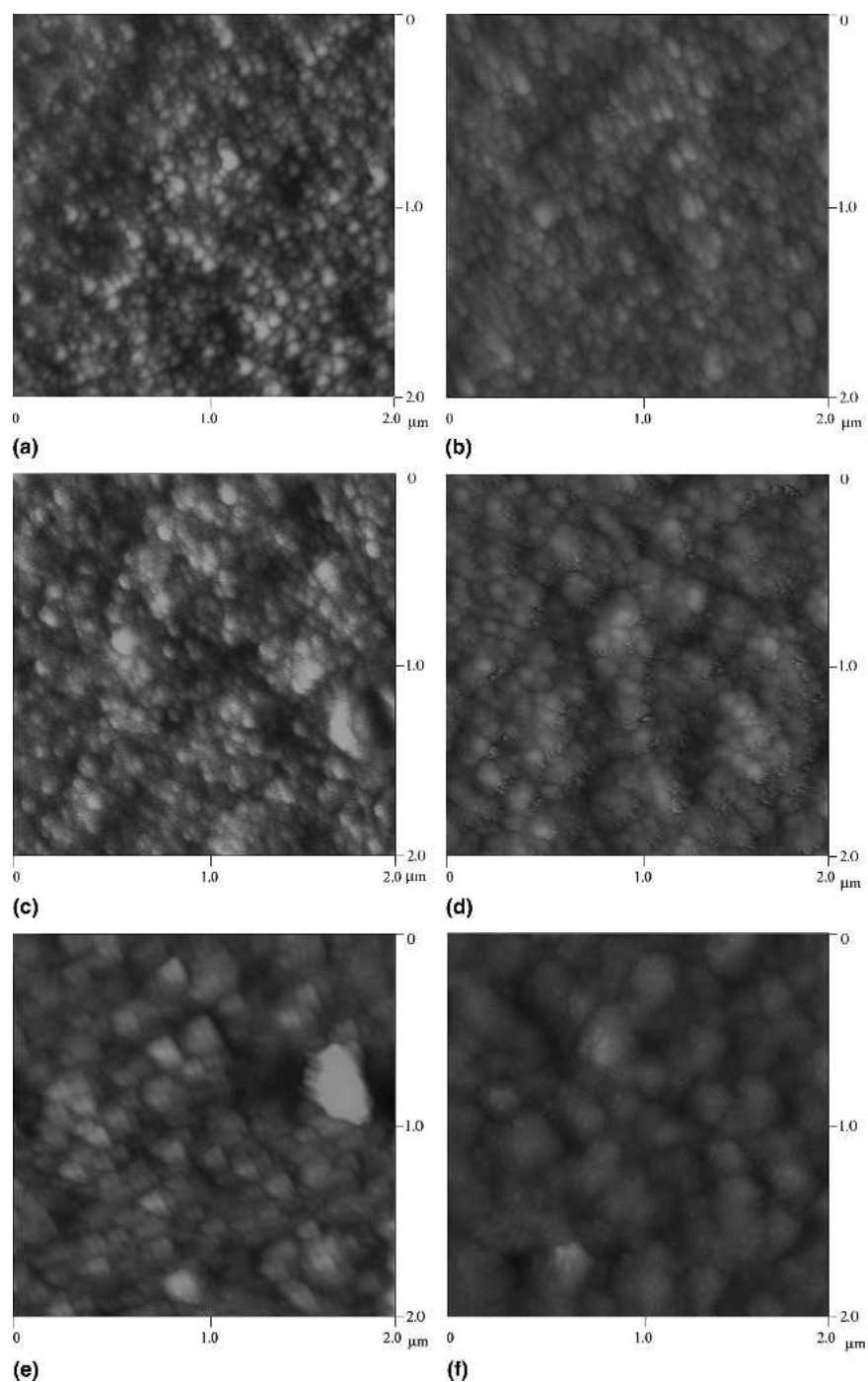


FIG. 4. AFM images of PEDOT/LiClO<sub>4</sub> coatings deposited on gold-coated sites with deposition charge from (a) to (f) of 1.8  $\mu\text{C}$ , 3.6  $\mu\text{C}$ , 7.2  $\mu\text{C}$ , 10.8  $\mu\text{C}$ , 21.6  $\mu\text{C}$ , and 43.2  $\mu\text{C}$ . The scanning length was 2  $\mu\text{m}$ .

mentioned above (512 nm). The maximum displacement for different PEDOT-coated sites having different coating thicknesses was in the range of 900 nm, corresponding to the deposition charge of 11  $\mu\text{C}$  (or deposition time of 30 min), whereas it was only 134 nm for a gold-coated silicon site under the same load. On the other hand, we found that the maximum displacement for PEDOT-coated sites began to decrease from 900 nm when the

deposition charge was above 11  $\mu\text{C}$ . These load versus displacement curves illustrate the much softer nature of conducting polymer compared with the harder silicon devices. The softer conducting polymer surface requires lower normal loads to induce a comparable indenter penetration.

As we have discussed above, the impedances of PEDOT-coated electrodes over the whole range of

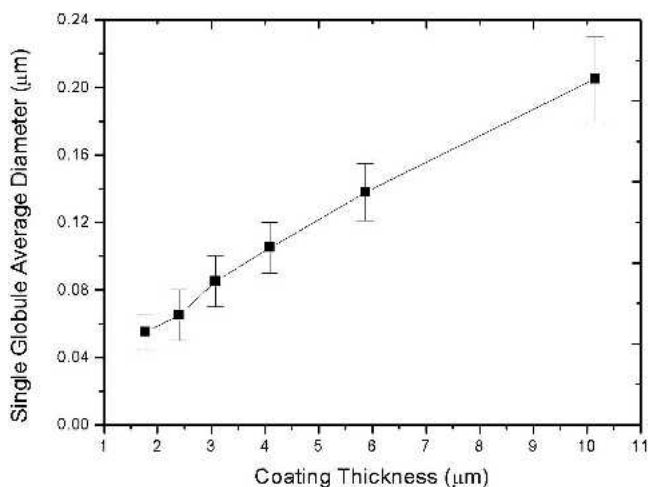


FIG. 5. The single globule average diameter of PEDOT/LiClO<sub>4</sub> coatings on gold-coated electrodes as a function of coating thickness.

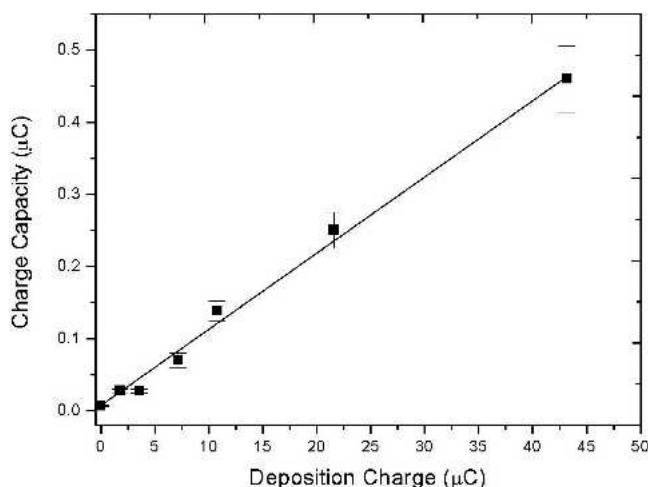


FIG. 7. The charge capacities of PEDOT/LiClO<sub>4</sub>-coated electrodes as a function of deposition charge.

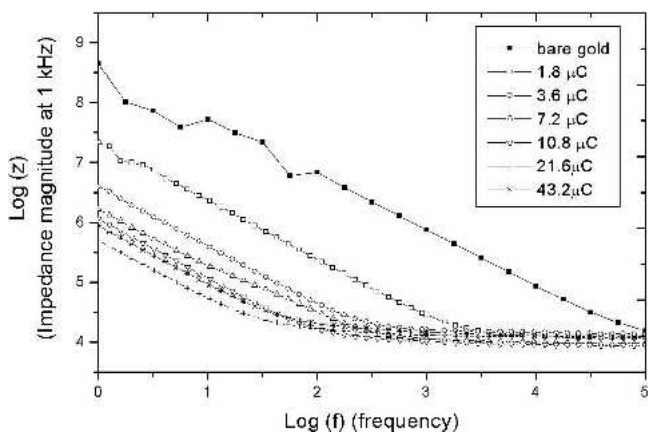


FIG. 6. Impedance spectroscopy of PEDOT/LiClO<sub>4</sub> electrodeposited on the electrodes (area is 1250 μm<sup>2</sup>) as a function of frequency compared with an uncoated gold electrode.

frequency (1–100 kHz) decreased with increasing frequency (Fig. 6). Because most neural activity is around 0.3 to 1 kHz, the impedance at 1 kHz has been used as a standard measure of the coated electrode quality.<sup>17</sup> Figure 9 shows the relationship between the coating thickness and impedance magnitude at 1 kHz for different PEDOT-coated electrodes. We can see that the impedance at 1 kHz decreased sharply after coating with PEDOT and continued to gradually decrease as the coating thickness increased (bold square curve in Fig. 9). The impedance dropped to a minimum at a coating thickness of about 4 μm (or 11 μC deposition charge), and then increased with increasing coating thickness. This correlated with increase in the effective area of the deposited polymer on the surface. Similar results have been found in our previous work.<sup>5,7,8</sup>

We found that the mechanical properties and electrical properties of PEDOT coatings varied in a systematic manner with coating thickness and surface morphology.

As can be seen from Fig. 9 (open square curve), the maximum displacement of the PEDOT-coated electrodes with different coating thicknesses correlates with impedance magnitude measured at 1 kHz. The displacement first increased and then decreased with increasing coating thickness. The lowest impedance of the PEDOT-coated electrode (solid square curve) at a coating thickness of about 4 μm is the coating that has the softest, largest displacement of 900 nm (open square curve), and thus has the most compliant mechanical response. In addition, the relationship between the hardness, the effective elastic modulus (stiffness), and the coating thickness are also shown in Fig. 10. We can see that the effective stiffness and the hardness decreased with increasing coating thickness, reaching a minimum at about a coating thickness of 4 μm, and then increased with a further increase in the coating thickness. They have the same trend as the relationships between the impedance magnitude at 1 kHz and coating thickness (Fig. 9, bold square curve). Therefore, our nanoindentation studies confirm that the PEDOT coatings on the electrode sites first become open and soft, and then stiffen and get more fully dense as the polymerization continues (Fig. 11). The lowest impedance films are those that have highest surface area and the softest, most compliant mechanical response. This is consistent with the interpretation that the high effective surface area of the films promotes the most facile charge transport.

To characterize the surface roughness as a function of coating thickness, the root mean square (RMS) roughness of PEDOT coatings deposited on electrode sites was calculated using NanoScope III software (version 5.12r3; Digital Instruments). The results in Fig. 12 show that the roughness of the coatings increased as the increase of coating thickness, reaching a maximum at a coating

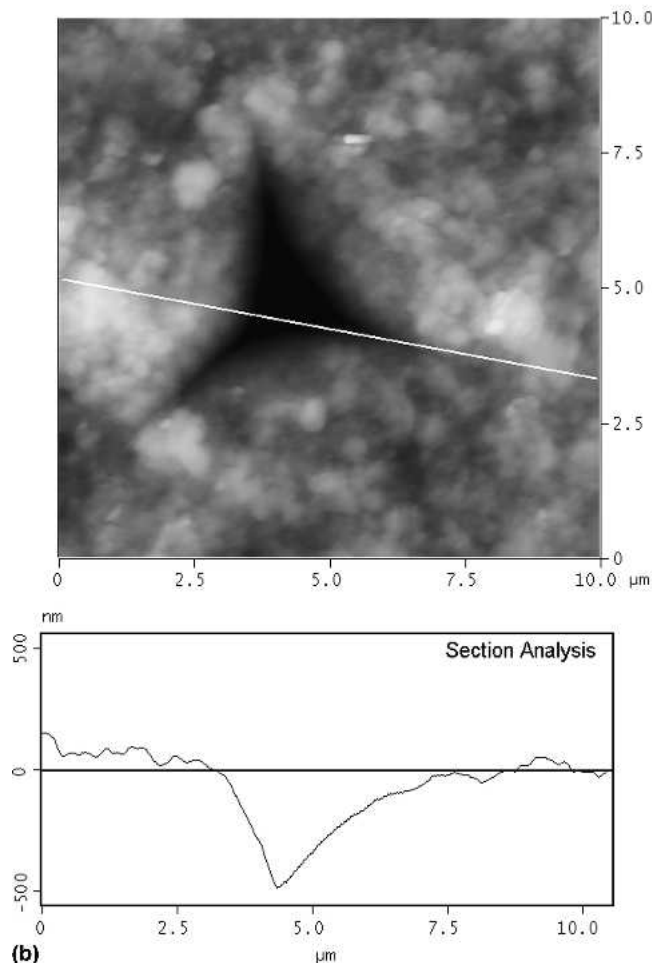
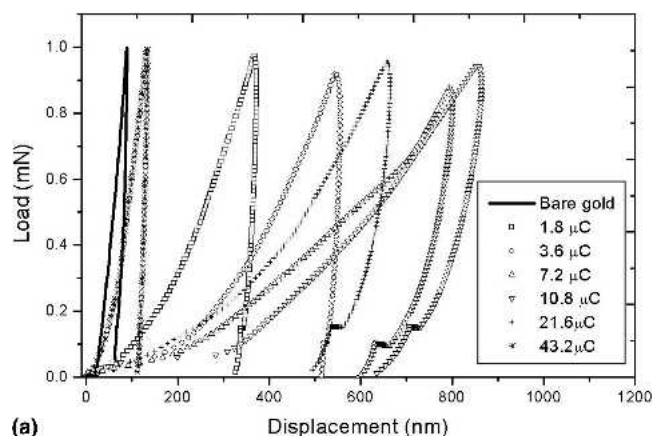


FIG. 8. (a) Load versus displacement curves for PEDOT/LiClO<sub>4</sub>-coated sites with different deposition charge (thickness) and (b) AFM indent image and section analysis of a selected site (corresponding to a deposition charge of 3.6 μC).

thickness of 4 μm, and then decreased sharply and followed by slower rate of increase as the increase of coating thickness. The results reveal that for highest rough surfaces of electrochemically polymerized PEDOT-coated electrodes, the minimum impedance also correlates well with the mechanical properties. The RMS just

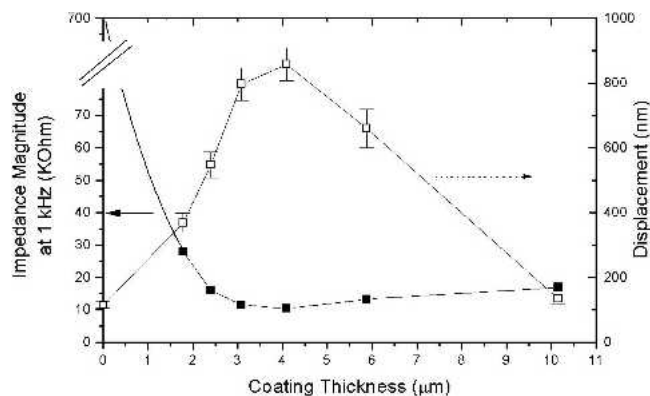


FIG. 9. The impedance magnitude at 1 kHz and the maximum displacement as a function of coating thickness. The displacements were obtained from nanoindentation tests with an applied load of 1 mN and a loading rate of 0.1 mN/s.

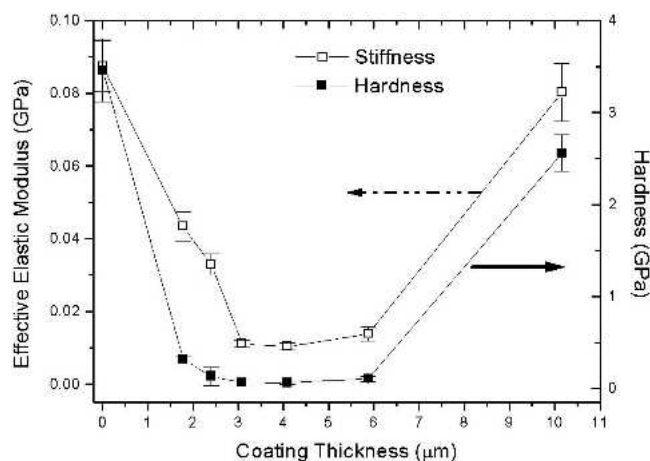


FIG. 10. The relationship between the coating thickness and the hardness and effective elastic modulus at an applied load of 1 mN with a loading rate of 0.1 mN/s.

gives a single value of roughness averaged over the length scale of observation, but does not demonstrate the length scale dependence of the surface roughness. Our previous work has reported a conducting polymer PPy electrochemically deposited on the electrode with fractal surface that can be quantitatively analyzed using power spectral density (PSD) method.<sup>18</sup> Figure 13 shows the PSD spectrum [log(PSD)~log(f) curves] of PEDOT coating taken from the 1.7-μm-thick film in Fig. 4. It shows a self-affine topography, and the two linear part of the plot (dash line) indicated that there were two different fractal regimes in this film. As can be measured from Fig. 13, the wave number at the transition point of PSD spectrum of 1.7-μm-thick PEDOT film is about 1.25 μm<sup>-1</sup>, corresponding to a wavelength of ~0.08 μm. The relationships between the wavelength and the coating thickness of PEDOT coatings are shown in Table I.

From the PSD analysis, it is possible to calculate the fractal dimension ( $D_s$ ) of the surface using a double logarithmic plot of spectral density versus wave number. The

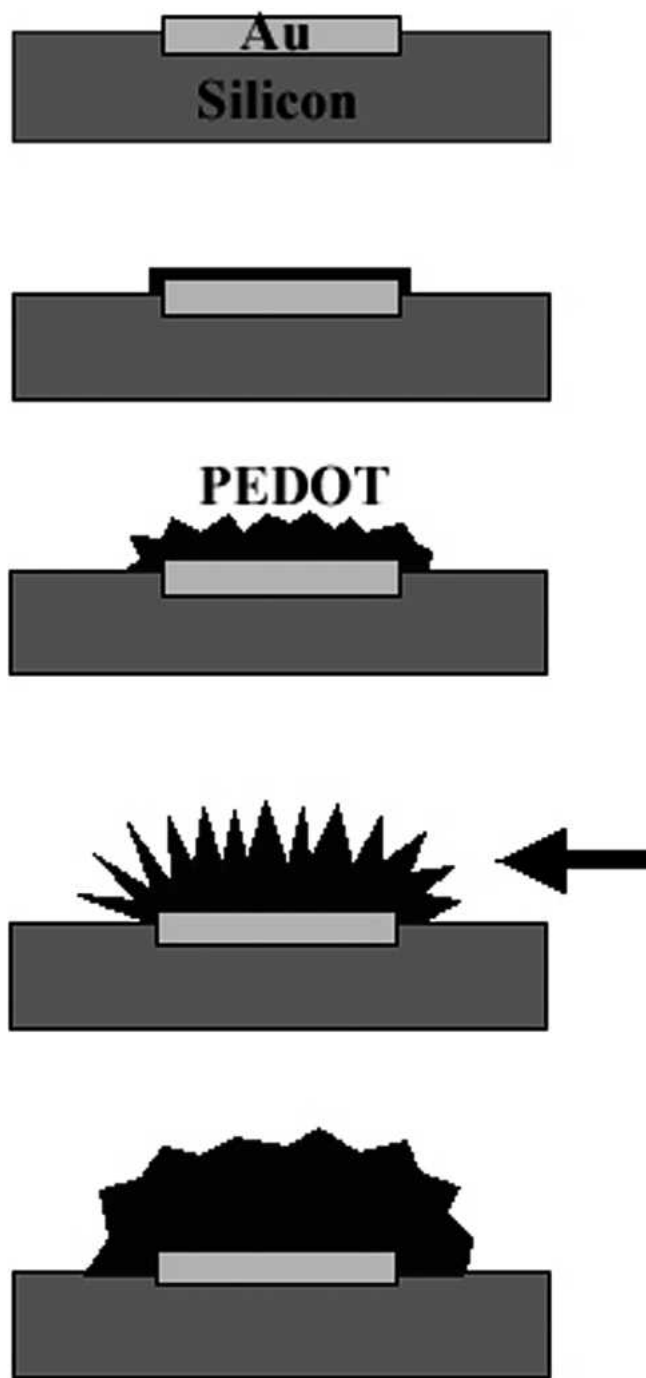


FIG. 11. Schematic illustration of surface morphology on electrode sites as a function of coating thickness (or deposition charge). The arrow shows that the electrode site has largest effective area corresponding to lowest impedance and softest coating.

$D_s$  represents a length-scale-invariant parameter related to the slope of the power spectral density of the surface,  $\beta$ , by

$$D_s = 0.5(7-\beta) \text{ [ref. 18-19] } .$$

The values of two effective  $D_s$  as a function of coating

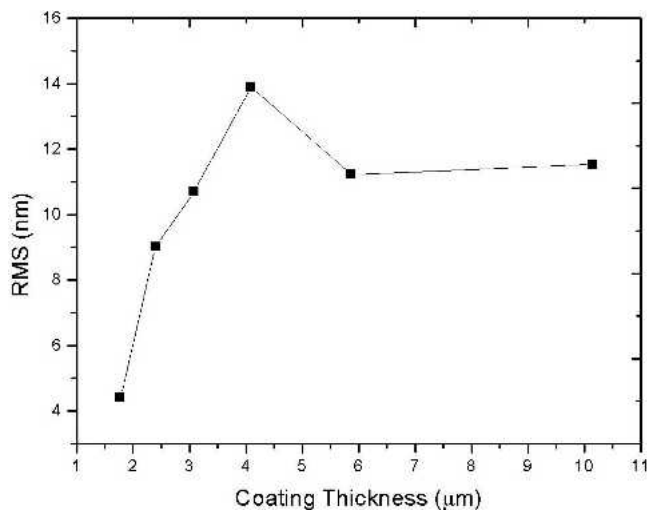


FIG. 12. The roughness (RMS) of different thicknesses of PEDOT/LiClO<sub>4</sub> coatings on gold-coated electrodes.

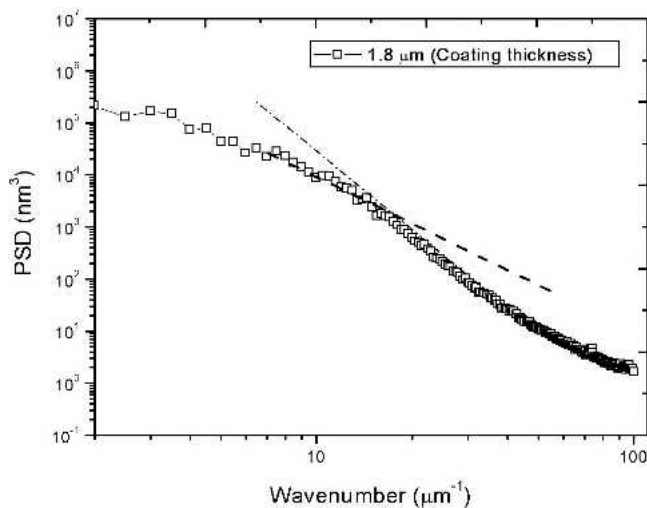


FIG. 13. PSD spectrum for 1.7-μm-thick PEDOT/LiClO<sub>4</sub> film electrochemically deposited on an electrode. The slope ( $\beta$ ) can be obtained from the curve-fitting equation.

TABLE I. The wavelength at transition point with different coating thickness.

Thickness (μm)	Deposition charge (μC)	Average wavelength at transition point (μm)
1.7	1.8	0.075
2.4	3.6	0.102
3.1	7.2	0.121
4.1	10.8	0.143
5.9	21.6	0.140
10.2	43.2	0.154

thickness are plotted in Fig. 14. In the high frequency range,  $D_s$  increased with increasing coating thickness, reaching a maximum at a thickness of 4 μm, and then decreased with further increase of the coating thickness.

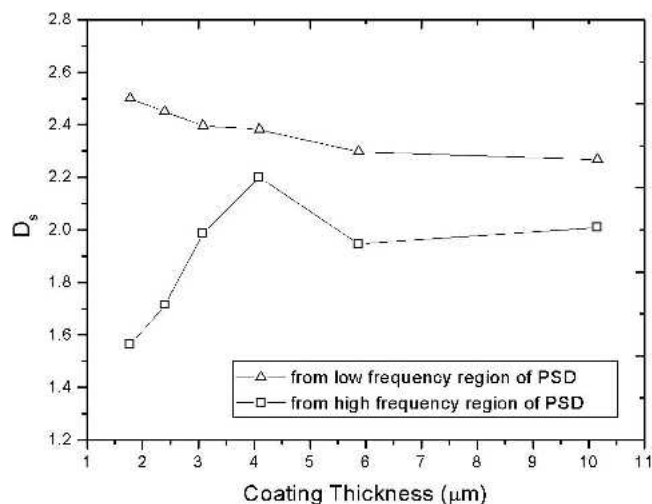


FIG. 14. The  $D_s$  calculated from PSD analysis of AFM images of different thickness PEDOT/LiClO<sub>4</sub> coatings on electrodes.

The results further confirm that the low frequency linear region of PSD was related to the roughness of the whole surface, whereas the high frequency part corresponded to the surface roughness of single globules (RMS). The PSD analysis was performed for  $2 \times 2$ - $\mu\text{m}$  images because, in this case, we have good spatial resolution for the single globules and the overall film surface structure. Correlations taken at other scan sizes such as  $5 \times 5$   $\mu\text{m}$  and  $10 \times 10$   $\mu\text{m}$  were not as consistent. These observations suggest that a critical length scale might be involved in the mechanisms of plasticity and charge transport, and that a more detailed study of surface geometry would be worthwhile in the future.

#### IV. CONCLUSIONS

The electrical properties and mechanical properties of conducting PEDOT/LiClO<sub>4</sub> coatings on electrode probes have been evaluated as a function of thickness by EIS and nanoindentation. These results have been compared with morphological studies by SEM and AFM. Our results reveal that for electrochemically deposited conducting PEDOT coatings on electrode sites, the minimum impedance correlates well with the surface microstructure and the mechanical properties. The lowest impedance films are those that have the highest surface area and roughness, and the most compliant mechanical response. The electrical and mechanical properties of these conducting polymer coatings are expected to have a strong influence on the long-term performance of microfabricated neural probes.

#### ACKNOWLEDGMENTS

This work was supported by NIH-NINDS-NO1-NS-1-2338. Partial support was also provided by the National

Science Foundation. The authors would also like to acknowledge the North Campus EMAL facility at the University of Michigan.

#### REFERENCES

1. C.J. Buchko, M.J. Slattery, K.M. Kozloff, and D.C. Martin: Mechanical properties of biocompatible protein polymer thin films. *J. Mater. Res.* **15**(1), 231 (2000).
2. A. Kros, S.W.F.M. van Hövell, N.A.J.M. Sommerdijk, and R.J.M. Nolte: Poly(3,4-ethylenedioxythiophene)-based glucose biosensors. *Adv. Mater.* **13**, 1555 (2001).
3. E. Smela: Conjugated polymer actuators for biomedical applications. *Adv. Mater.* **15**(6), 481 (2003).
4. H. Yamato, M. Ohwa, and W. Wernet: Stability of polypyrrole and poly(3,4-ethylenedioxythiophene) for biosensor application. *J. Electroanal. Chem.* **397**, 163 (1995).
5. X.Y. Cui and D.C. Martin: Electrochemical deposition and characterization of poly(3,4-ethylenedioxythiophene) on neural micro-electrode arrays. *Sens. Actuators B Chem.* **89**, 92 (2003).
6. J. Yang and D.C. Martin: Microporous conducting polymers on neural prosthetic devices. I. Electrochemical deposition. *Sens. Actuators B Chem.* **101**, 133 (2004).
7. J. Yang and D.C. Martin: Microporous conducting polymers on neural prosthetic devices. II. Physical characterization. *Sens. Actuators A Phys.* **113**, 72 (2004).
8. J. Yang, D.H. Kim, J.L. Hendricks, M. Leach, R. Northey, and D.C. Martin: Ordered surfactant-templated poly(3,4-ethylenedioxythiophene) (PEDOT) conducting polymer on microfabricated neural probes. *Acta Biomaterialia* **1**, 125 (2005).
9. X.S. Wang and X.Q. Feng: Effects of thickness on mechanical properties of conducting polythiophene films. *J. Mater. Sci. Lett.* **21**, 715 (2002).
10. X.S. Wang, J.K. Xu, G.Q. Shi, and X. Lu: Microstructure-mechanical properties relationships in conducting polypyrrole films. *J. Mater. Sci.* **37**, 5171 (2002).
11. H. Yamato, K-I. Kai, M. Ohwa, W. Wernet, and M. Matsumura: Mechanical, electrochemical and optical properties of poly(3,4-ethylenedioxythiophene)/sulfated poly( $\beta$ -hydroxyethers) composites films. *Electrochim. Acta* **42**, 2517 (1997).
12. B.J. Briscoe, L. Fiori, and E. Pelillo: Nanoindentation of polymeric surface. *J. Phys. D: Appl. Phys.* **31**, 2395 (1998).
13. T.H. Fang and W.J. Chang: Nanoindentation characteristics on polycarbonate polymer film. *Microelectron. J.* **35**, 595 (2004).
14. B.D. Beake and G.J. Leggett: Nanoindentation and nanoscratch testing of uniaxially and biaxially drawn poly(ethylene, terephthalate). *Polymer* **43**, 319 (2002).
15. P.V. Pavoov, A. Bellare, A. Strom, D. Yang, and R.E. Cohen: Mechanical characterization of polyelectrolyte multilayers using quasi-static nanoindentation. *Macromolecules* **37**, 4865 (2004).
16. W.C. Oliver and G.M. Pharr: An improved technique for determining hardness and elastic modulus using load and displacement sensing indentation experiments. *J. Mater. Res.* **7**, 1564 (1992).
17. S.W. Kuffler: *From Neuron to Brain: A Cellular Approach to the Function of the Nervous System*. (Sinauer Associates, Sunderland, MA, 1976).
18. X. Cui, J.F. Jetke, J.A. Wiler, D.J. Anderson, and D.C. Martin: Electrochemical deposition and characterization of conducting polymer polypyrrole/PSS on multichannel neural Probes. *Sens. Actuators A Phys.* **93**, 8 (2001).
19. C.J. Buchko, K.M. Kozloff, and D.C. Martin: Surface characterization of porous, biocompatible protein polymer thin films. *Biomaterials* **22**, 1289 (2001).